The impact of demographic changes on the epidemiology of Herpes Zoster: Spain as a case study

Valentina Marziano[1,2], Piero Poletti[1,3], Giorgio Guzzetta[1,4], Marco Ajelli[1], Piero Manfredi[5] and Stefano Merler[1]

[1] Center for Information Technology, Bruno Kessler Foundation, Trento, Italy,
[2] Department of Mathematics, University of Trento, Trento, Italy,
[3] DONDENA Centre for Research on Social Dynamics, Bocconi University, Milan, Italy,
[4] Trento Rise, Trento, Italy,
[5] Department of Statistics and Mathematics Applied to Economics, University of Pisa, Pisa, Italy.

Supplementary Material

Contents

1 The model

In this study we use a stochastic individual-based model for Varicella-Zoster Virus (VZV) transmission and reactivation. Full details are provided hereafter.

1.1 Description

The population is stratified by 101 one-year age classes, $a \in \{0, 1, 2, ..., 99, 100+\}$. The model accounts for the vital dynamics of the Spanish population, by considering yearly variations in birth rate, mortality rates and migration fluxes. All individuals are born susceptible to VZV and acquire varicella with a time-dependent, age-specific force of infection (FOI) defined as:

$$\lambda_j(t) = \beta \sum_k C_{jk}(t) y_k(t) \tag{1}$$

where

- $\lambda_j(t)$ is the FOI for age class j at time t;
- β is the VZV transmission rate;
- $C_{jk}(t)$ is the contact matrix at time t, defined as the number of contacts of an individual in the age group j with individuals in the age group k. More specifically, it is computed at each time as $C_{jk}(t) = \tilde{C}_{jk}\pi_k(t)$, where estimates for contacts provided in [1], $\tilde{C}_{jk}$, are rescaled by the current fraction of individuals in the age group k over the total population, $\pi_k(t)$.
- $y_k(t)$ is the fraction of varicella-infectious individuals within the age group k at time t;

This form of the FOI was previously proposed in the classical modelling literature for measles [2, 3] and theoretically analysed [4] in the context of demographic changes. In formulation (1), we neglect the contribution of Herpes Zoster (HZ) infected individuals to the FOI, based on the observation that HZ is less infectious and much less frequent than varicella [5]. VZV infected individuals recover at a constant rate γ. Once recovered from varicella, individuals gain lifelong immunity to VZV reinfection and become susceptible to HZ. The risk of developing HZ is reduced by subsequent re-exposures to VZV infectious individuals, called boosting events, that occur at a rate proportional to the FOI through a coefficient $z \in [0, 1]$. This coefficient represents the assumption that only a fraction z of the contacts that would result in varicella infection in susceptibles triggers a boosting of the immune response against HZ.
HZ susceptible individuals reactivate VZV, thus developing HZ, according to a risk that depends on the number of VZV exposure episodes i, on the age of the host a and on the time elapsed since last VZV exposure τ. In particular, we assume the same functional form as in [6]:

$$\rho_i(a, \tau) = \rho_0 q^{(i-1)^2} e^{\theta_a (a-a_0)^+} e^{\theta_\tau \tau} \tag{2}$$

where

- $\rho_i(a, \tau)$ is the VZV reactivation risk;
- the term $q^{(i-1)^2}$, where $q \in [0, 1]$, accounts for the reduction of HZ risk when the number of VZV exposures increases ($i = 1$ represents primary varicella infection);
- the exponential term $e^{\theta_a (a-a_0)^+}$, where $\theta_a > 0$ and $(a - a_0)^+ := \max(0, a - a_0)$, accounts for the increase of HZ risk due to immunosenescence of the host [7]. We assume that aging begins to have an effect on the risk of reactivation starting from age $a_0 = 45$ years [8, 6];
- the exponential term $e^{\theta_\tau \tau}$, where $\theta_\tau > 0$, accounts for the increase of HZ risk as the time elapsed since last VZV exposure episode increases;
- ρ_0 is the risk of developing HZ for individuals younger than 45 years of age ($a < a_0$), who have just recovered from varicella infection ($\tau = 0$, $i = 1$).

Individuals who have developed HZ are assumed to become permanently immune to VZV reactivation, based on the fact that recurrent HZ is relatively uncommon in immunocompetent persons [9], as detailed in the Methods section in the main text.
A schematic representation of the model is given in Figure S1.

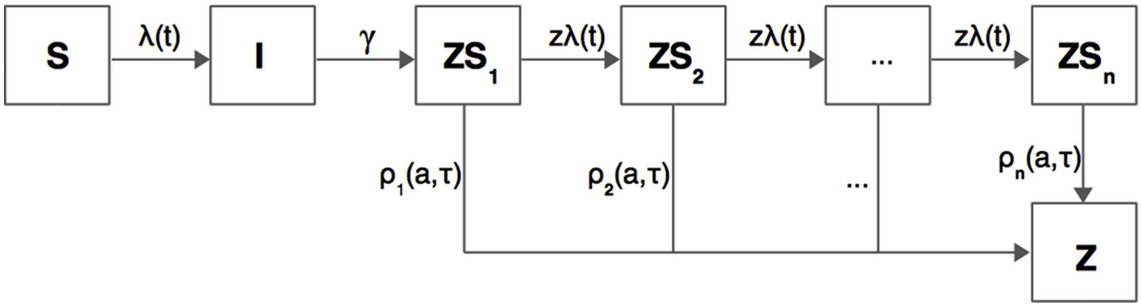

Figure S1: **Flow diagram of the model. Varicella and HZ.** S: VZV susceptible individuals; I: varicella infectious individuals; $ZS_1, ZS_2, ..., ZS_n$: HZ susceptible individuals with respectively $1, 2, ..., n$ episodes of previous exposure to VZV; Z: individuals who have developed HZ. $\lambda(t)$: time-dependent force of infection, γ: constant recovery rate from varicella, z: boosting efficacy and $\rho_1(a, \tau)$, $\rho_2(a, \tau)$, ..., $\rho_n(a, \tau)$: VZV reactivation rates.

The model requires the tracking of HZ susceptibility states by age, time since last exposure to VZV and cumulative number of re-exposures. Considering 100 one-year age groups, a mean number of lifetime re-exposures of about 7 (see Section 3) and a yearly discretization for the time since last exposure, the number of possible states for individuals susceptible to HZ amounts to at least $7 \times 100 \times 100/2 = 35,000$ (division by 2 accounts for the time since last exposure being always smaller than chronological age), which possibly underestimates the actual number of states, since some individuals may experience more than 7 re-exposure episodes. In this study, the considered population size replicates the one on which the HZ calibration dataset was collected (the region of Navarra, about 600,000 individuals in 2009). Comparing population

size with the number of HZ susceptibility states, it results that the mean population in each state is smaller than $600,000/35,000 \approx 17$. This number gets even smaller if we consider the possible underestimate of the number of HZ susceptibility states, that the models population at the beginning of the century was about 1/3 of the current one, that not all individuals are HZ susceptibles and that the distribution of the population across model states is not homogeneous. Deterministic models assume a continuous variable for the population size over the various structural dimensions (represented here by chronological age, age since last exposure, and number of exposures): such assumption is only valid for a sufficiently large number of individuals in each compartment. For these reasons we preferred a stochastic individual-based model over a deterministic one.

1.2 Simulation algorithm

For each individual we take into account:

- age a, measured in years, $a \in \{0, ..., 100\}$;
- epidemiological status:= $\begin{cases} \text{Susceptible to VZV} \\ \text{Infected by varicella} \\ \text{HZ susceptible} \\ \text{Infected or recovered from HZ} \end{cases}$
- number of VZV exposures $\begin{cases} i = 0 & \text{Varicella susceptible individual} \\ i = 1 & \text{Primary varicella infection} \\ i > 1 & \text{Subsequent boosting episodes} \end{cases}$
- a^*, age of the individual at the time of last VZV exposure occurrence.

Time is discretized using a step of 1 week. At each time step the following events occur:

- Recoveries: the number of recoveries is obtained by sampling a Poisson distribution with parameter γI, where γ is the recovery rate and I is the current total number of infectious individuals.
- Primary varicella infections: the number of varicella infections is obtained, for each age group j, by sampling a Poisson distribution with parameter $\lambda_j S_j$ where λ_j is defined in Eq. (1) and S_j is the current total number of susceptibles in age group j. For each infected individual, i is set to 1 and a^* is updated with his current age.
- Boosting events: the number of boosting events is obtained, for each age group j, by sampling a Poisson distribution with parameter $z\lambda_j ZS_j$, where z is the parameter which accounts for boosting efficacy, λ_j is defined in Eq. (1) and ZS_j is the current total number of HZ susceptibles in age group j. For each boosted individual, i is incremented by 1 and a^* is updated with his current age.

- Births: the number of births is obtained by sampling a Poisson distribution with parameter $bN/52$, where b, N denote respectively the crude birth rate for the current year and the current total population.

The following events occur at a yearly frequency (at the end of each year):

- VZV reactivations: for each HZ susceptible individual with i VZV exposure episodes, age a, and time since last exposure $\tau = a - a^*$, VZV reactivation may occur according to a Bernoulli sample with probability $\rho_i(a, \tau)$, defined in Eq. (2).

- Deaths: for each individual of age a death may occur according to a Bernoulli sample with probability $\mu(a)$, representing age-specific mortality rate for the current year. $\mu(a)$ is obtained as the weighted mean of male- and female-specific mortality rates for age a, where the weight is the sex ratio.

- Migrations: a number of individuals is added or removed from the population based on the relative age-specific migration flux for the current year. In the case of a positive migration rate, the epidemiological status of added individuals is assigned according to the current epidemiological profile in the resident population.

- Aging: at the end of each year the age of all individuals is incremented by 1, with the exception of those belonging to the age class $a = 100$.

1.3 Model inputs

The model takes as input the following data:

- yearly birth rates [10] for the time period considered in the simulation (shown in Figure 1, main text);

- annual sex- and age-specific mortality rates [11] for the considered period (Figure S2**a-b**);

- yearly migration fluxes [12, 13] (Figure S2**c**);

- age structure of the migrant population [14];

- age-specific contact matrix estimated for Spain in [1].

2 Model calibration

The model has six free parameters:

- the VZV transmission rate β;

- four parameters defining the VZV reactivation rate: $\rho_0, \theta_a, \theta_\tau, q$ (see Eq. (2));

- the boosting efficacy z.

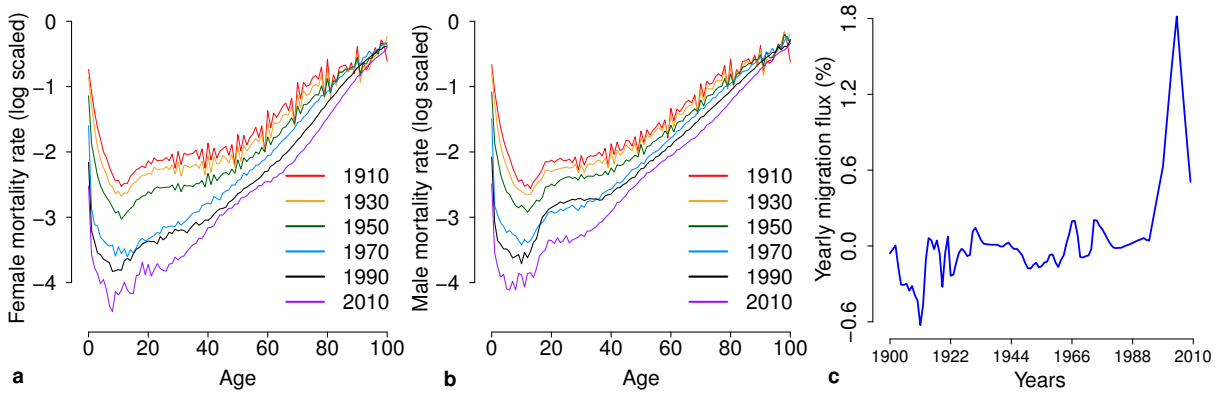

Figure S2: **Historical demographic data.** **a** Age-specific mortality rate, females [11]. **b** Age-specific mortality rate, males [11]. **c** Yearly migration flux in % of the population [12, 13]

The parameter vector is defined as $\Theta = (\beta, \rho_0, \theta_a, \theta_\tau, q, z)$. The posterior distribution of parameters was explored by using Markov Chain Monte Carlo (MCMC) applied to the likelihood of observed data, using uniform prior distributions. The likelihood is defined as the product between the binomial likelihood $\mathcal{L}_A$ of the observed VZV serological profile by age in 1996 [15] and the Poisson likelihood $\mathcal{L}_B$ of the observed HZ incidence profile by age in 2005-2006 [16]. Specifically,

$$\mathcal{L}_{\mathcal{A}}(n_m, r_m|\Theta) = \prod_{m=1}^{M} \frac{n_m!}{r_m!(n_m - r_m)!}(p_m(\Theta))^{r_m}(1 - p_m(\Theta))^{n_m - r_m} \tag{3}$$

where

- M is the number of ages considered in the serological profile [15];
- n_m is the number of individuals of age m observed in [15];
- r_m is the number of seropositive individuals of age m observed in [15];
- $p_m(\Theta)$ is the VZV seroprevalence for age m, simulated by the model in 1996 with parameter set Θ.

and

$$\mathcal{L}_B(k_j|\Theta) = \prod_{j \in J} \frac{e^{-\eta_j(\Theta)}(\eta_j(\Theta))^{k_j}}{k_j!} \tag{4}$$

where

- J is the set of age groups in the HZ incidence profile [16];
- k_j is the total number of HZ cases in the j-th age group observed in [16];

- $\eta_j(\Theta)$ is the number of HZ cases in the age group j, simulated by the model in 2005-2006 in a population of the same size as that analyzed in [16], with parameter set Θ.

We determined the posterior distribution of Θ using random-walk Metropolis-Hastings sampling [17]. At each iteration, the algorithm evaluates the likelihood of a new candidate vector of parameters, that is accepted or not based on the standard Metropolis-Hastings algorithm. The values of a new candidate parameter vector are randomly sampled from normal distributions having mean equal to the current values and standard deviations given in Table S1. The algorithm is

Table S1: **Standard deviations for parameters.**

Parameter	Standard Deviation	Range
β	$4.3 \cdot 10^{-2}$	$[0, +\infty)$
ρ_0	$7.0 \cdot 10^{-5}$	$[0, +\infty)$
θ_a	$8.8 \cdot 10^{-3}$	$[0, +\infty)$
θ_τ	$4.3 \cdot 10^{-3}$	$[0, +\infty)$
q	$6.3 \cdot 10^{-2}$	$[0, 1]$
z	$2.4 \cdot 10^{-2}$	$[0, 1]$

run for 22,000 iterations and a burn-in period of 2,000 iterations is considered. Convergence is checked by considering several different starting points and by visual inspection. Estimated mean values and 95%CI of parameters are reported in Table S2. The reported mean values and credible intervals are computed from the selected realizations of the model, and thus account for both the stochasticity of model realizations and the uncertainty in model parameters estimates.

Table S2: **Estimates of parameters obtained for Spain.**

Parameter	Description	Mean	Unit	95% CI
β	VZV transmission rate	1.02×10^5	weeks^{-1}	$0.95 \times 10^5, 1.10 \times 10^5$
ρ_0	HZ risk at birth [1]	2.63×10^{-3}	years^{-1}	1.96×10^{-3} , 3.21×10^{-3}
θ_a	Rate of risk exponential growth with chronological age a [1]	11.19×10^{-2}	years^{-1}	7.53×10^{-2} , 14.53×10^{-2}
θ_τ	Rate of risk exponential growth with time since last exposure τ [1]	4.77×10^{-2}	years^{-1}	3.89×10^{-2} , 5.81×10^{-2}
q	Parameter regulating HZ risk reduction with increasing number of re-exposures to VZV [1]	0.64		0.46 , 0.81
z	Boosting efficacy	0.73		0.64 , 0.83

[1] $\rho_i(a, \tau) = \rho_0 q^{(i-1)^2} e^{\theta_a (a-a_0)^+} e^{\theta_\tau \tau}$

3 Additional results

3.1 Historical period (1900-2009)

The model is able to correctly reproduce the observed evolution of the population age structures [10], as shown in Figure S3. The curves show downward peaks, reflecting the brisk drop of birth

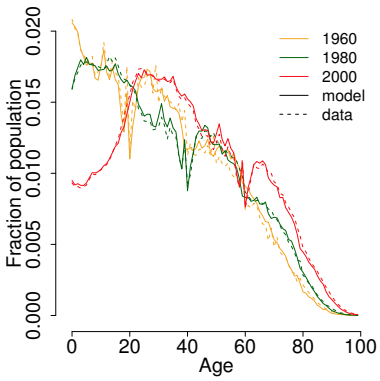

Figure S3: Age distribution of the population at different years as observed [10] (dotted lines) and as predicted by the model (solid lines).

rate (Figure 1, main text) during the Spanish Civil War (1936-1939).
The remarkable changes in the population age structure shown above have led, according to the model, to a reduction of VZV circulation. This has produced a reduction over time of the estimated mean number of VZV re-exposures collected by HZ susceptibles (Figure S4), that has led to the increase in HZ incidence (Figure 3**c** in the main text).

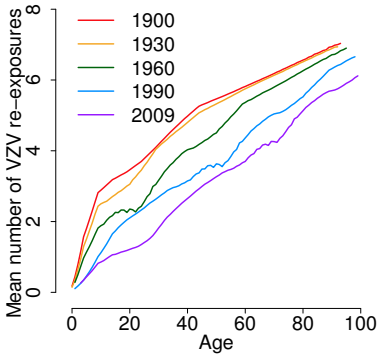

Figure S4: Estimated mean number of VZV re-exposures by age at different years.

3.2 Prediction scenarios (2010-2050)

In this section we discuss further results obtained for the illustrative scenarios presented in the main text for Spain and results obtained for an official demographic projection scenario based on the 2012 UN population prospects [18].

Illustrative scenarios

The predicted evolution of the age structure of the Spanish population in the "Lowest-birth rate" (L, Figure 1 in the main text) and"Highest-birth rate" (H, Figure 1 in the main text) scenarios are shown in Figures S5**a** and S5**c**. Scenario L is characterized by a remarkable aging of the population, whereas in scenario H the fraction of young individuals in the population is predicted to increase. Such changes lead respectively to a decrease (scenario L) and to an increase (scenario H) of VZV circulation, that influences the age-specific number of boosting events within the population. In particular, as shown in Figure S5**b**, in scenario L the mean number of boosting events by age is predicted to decrease during the period 2010-2050 and this explains the predicted strong increase in HZ (see Figure 5**c** in the main text). On the other hand, as shown in Figure S5**d**, the increasing VZV circulation in scenario H leads to an increase of the mean number of VZV re-exposures for young people and adults, which partially mitigates the HZ increase caused by demographic changes occurred during the last century (see Figure 5**d** in the main text).

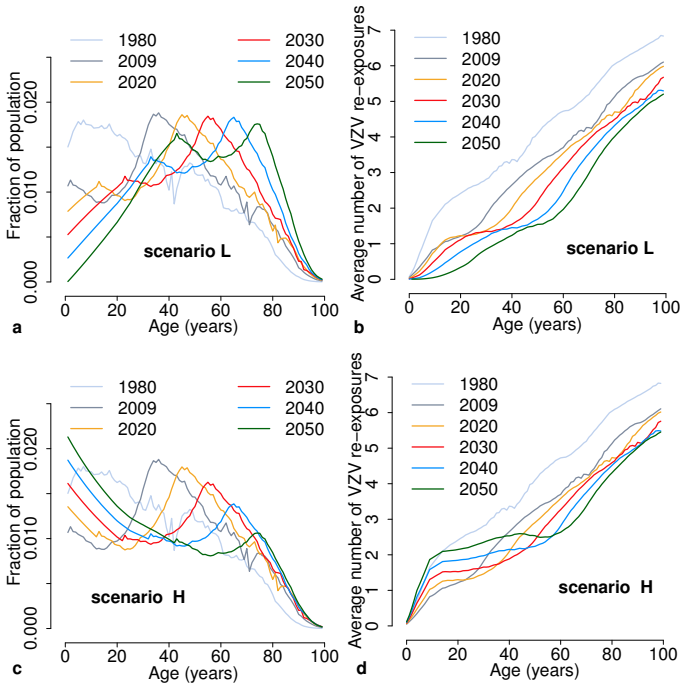

Figure S5: **a** Age distribution of the population at different years in scenario L. **b** Mean number of VZV re-exposures by age at different years in scenario L. **c** As **a** but for scenario H. **d** As **b** but for scenario H.

Scenario based on UN demographic projections

In addition to the illustrative scenarios proposed in the main text we considered an official demographic projection scenario for Spain, based on the medium variant of the 2012 UN population

prospects [18]. This scenario predicts an initial decrease followed by a recovery of the birth rate between 2010 and 2050 (see Figure 1 in the main text) and a progressive decrease of migration fluxes and mortality rates, especially in the elderly, during the same period.
As shown in Figure S6, results obtained for this scenario are quite similar to the baseline, which assumes constant birth, mortality and migration rates for the whole prediction period. This is because the variation in the birth rate predicted during the period 2010-2050 by the realistic scenario considered is negligible when compared to that experienced during the last century and HZ dynamics are much less sensitive to changes in migration fluxes and mortality rates in adults and older individual, as they do not impact significantly on age groups involved in varicella transmission.
In summary, even under realistic demographic projections, an increase of HZ incidence should be expected in Spain as a consequence of the dramatic demographic changes that characterized the last century.

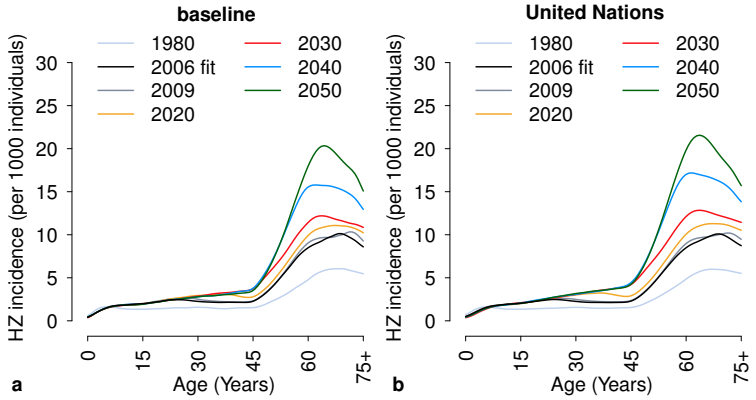

Figure S6: **Predicted HZ incidence in Spain (2010-2050). Comparison between baseline and realistic scenario. a** Age-specific HZ incidence predicted by the model at different years for the baseline scenario. **b** As **a** but fot the demographic scenario based on UN population prospects [18].

4 Vaccination

In addition to results provided in the main text, we report in Figure S7 the total incidence of varicella and HZ over time under a vaccination program starting in 2010 and targeting children of 15 months of age, considering different scenarios for the combined value of coverage and efficacy: 80%, 90% and 100%. The Figure shows that coverage does not significantly affect the HZ incidence; however coverage at 80% is not sufficient to provide elimination of varicella in the long term.

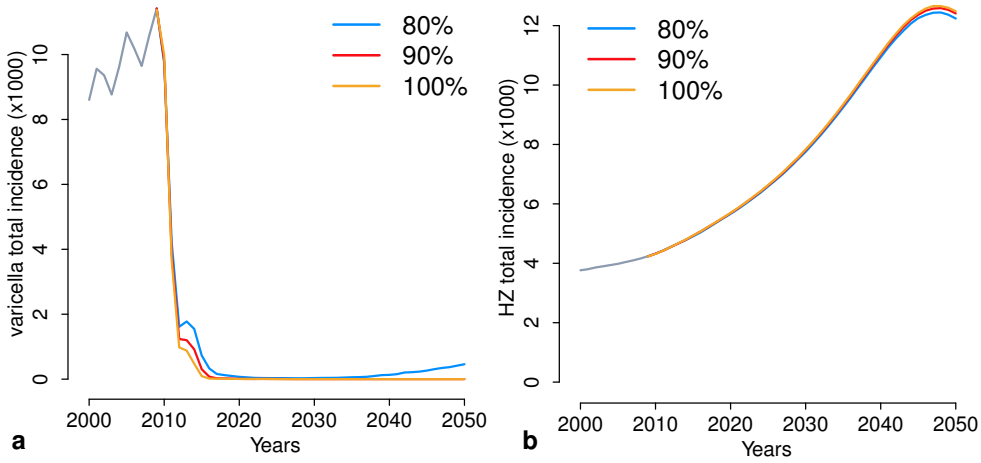

Figure S7: **Model predictions under a vaccination program starting in 2010 and for different scenarios for the combined value of vaccine efficacy and coverage. a** Total varicella incidence over time. **b** Total HZ incidence over time.

5 Homogeneous mixing

To provide a comparison of model results under a different assumption on mixing patterns, we recalibrated the model by assuming homogeneous mixing (i. e. $C_{jk}(t) = 1$). We show that the model behavior is qualitatively similar to that reported in the main text, with a reduction over the past century of VZV circulation (Figure S8**a**) and a growth in the mean age at varicella (S8**b**), total and age-specific HZ incidence (S8**c** and inset) and mean age at VZV reactivation (S8**d**). In particular, under the homogeneous mixing assumption, the predicted growth of the total HZ incidence between 1997 and 2004 is higher (about 18%) than that predicted using age-specific contact matrices (about 12%). We conclude that the HZ growth predicted as a consequence of demographic changes is robust under different assumptions on mixing patterns.

6 A different formulation of exogenous boosting

The model was also recalibrated using a different formulation of the exogenous boosting hypothesis. In this alternative formulation, the mechanism of VZV reactivation is modeled as in [19, 20, 21]. In particular, once recovered from varicella individuals acquire lifelong immunity to varicella and temporary immunity to HZ. After an average time of $1/\delta$ the protection against HZ wanes and individuals become susceptible to VZV reactivation. HZ susceptibles may either be boosted or develop HZ. The risk of VZV reactivation has the following functional form [19]:

$$\rho(a) = \omega e^{-\phi a} + a^{\eta}\pi \qquad \omega, \phi, \eta, \pi > 0$$

The model is schematically described in Figure S9.
Results obtained are, again, qualitatively analogous to those shown in the main text, with an

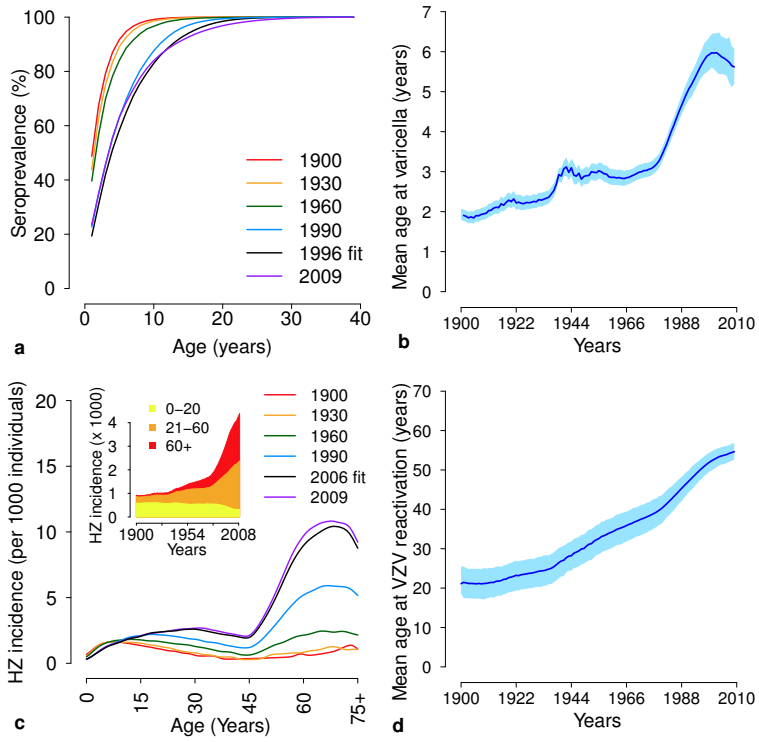

Figure S8: **Estimated impact of demographic changes on VZV epidemiology by assuming homogeneous mixing. Historical period (1900-2009). a** Estimated age-specific VZV seroprevalence at different years. **b** Estimated mean age (and 95%CI, shaded areas) at varicella over time. **c** Estimated age-specific HZ incidence at different years. The inset shows the total HZ incidence over time and disaggregated by age group. **d** Estimated mean age (and 95%CI, shaded areas) at HZ over time.

increasing trend in the estimated total HZ incidence (Figure S10**a**) over the last century. In this case, the estimated growth is smaller than that predicted by the progressive immunity model (reproposed here for convenience, Figure S10**b**). We conclude, that the HZ growth predicted as a consequence of demographic changes is robust under different model formulations of exogenous boosting.

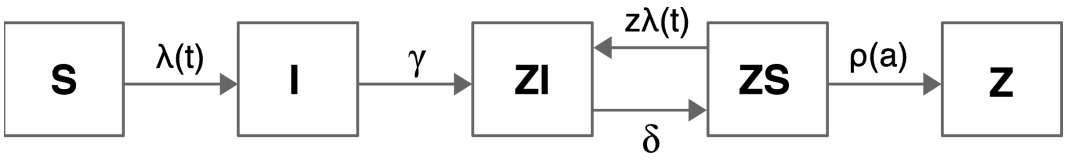

Figure S9: **Flow diagram of the model based on [19].** S: VZV susceptible individuals; I: varicella infectious individuals; ZI: individuals immune to HZ and VZV infection; ZS: HZ susceptibles individuals; Z: individuals who have developed HZ. $\lambda(t)$: time-dependent force of infection, γ: constant recovery rate from varicella, z: boosting efficacy, $1/\delta$: duration of immunity to HZ after exposure to varicella and $\rho(a)$: VZV reactivation rate.

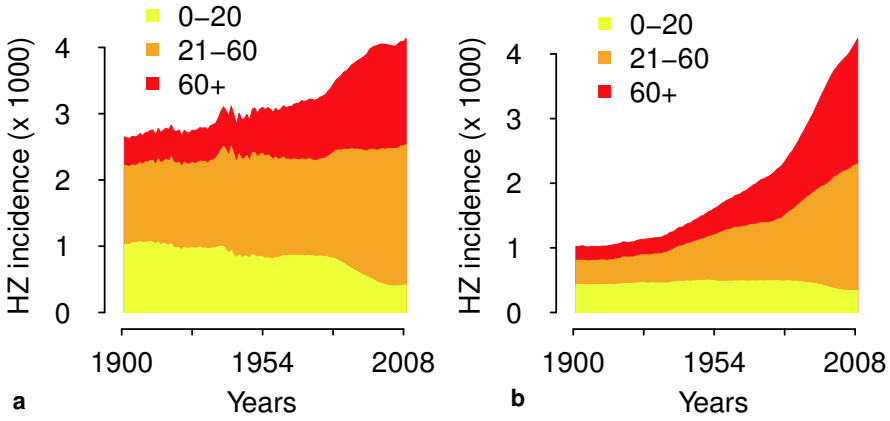

Figure S10: **Total HZ incidence and disaggregated by age group.** **a** As predicted by the alternative model formulation based on a mechanism of temporary immunity. **b** As predicted by progressive immunity model.

References

[1] Fumanelli L, Ajelli M, Manfredi P, Vespignani A, Merler S. Inferring the structure of social contacts from demographic data in the analysis of infectious diseases spread. PLOS Comput Biol 2012;8(9):e1002673.

[2] Mc Lean AR, Anderson RM. Measles in developing countries. Part I. Epidemiological parameters and patterns. Epidemiol Infect. 1988;100:111.

[3] De Jong M, Diekmann O, Heesterbeek H. How does transmission of infection depend on population size? In: Mollison D, editor. Epidemic Models. Cambridge University; 1995. p. 84.

[4] Manfredi P, Williams JR. Realistic population dynamics in epidemiological models: the impact of population decline on the dynamics of childhood infectious diseases. Measles in Italy as an example. Math Biosci 2004;192:153–175.

[5] Seiler HE. A study of Herpes Zoster particularly in its relationship to chickenpox. J Hyg 1949;47(3):253–262.

[6] Guzzetta G, Poletti P, dal Fava E, Ajelli M, Scalia Tomba G, Merler S, et al. Hope-Simpson's progressive immunity hypothesis as a possible explanation for herpes zoster incidence data. Am J Epidemiol 2013;177(10):1134–1142.

[7] Burke BL, Steele RW, Beard OW, Wood JS, Cain TD, Marmer DJ. Immune Responses to Varicella-Zoster in the Aged. Arch Intern Med 1982;142(2):291–293.

[8] Karhunen M, Leino T, Salo H, Davidkin I, Kilpi T, Auranen K. Modelling the impact of varicella vaccination on varicella and zoster. Epidemiol Infect 2010;138:469–481.

[9] Oxman MN. Herpes Zoster Pathogenesis and Cell-Mediated Immunity and Immunosenescence. The Journal of the American Osteopathic Association. 2009 June;109(6).

[10] Instituto Nacional de Estadistica; [cited 29 December 2014]. Available from: http://www.ine.es/.

[11] Human Mortality Database. University of California, Berkeley (USA) and Max Planck Institute for Demographic Research (Germany); [cited 29 December 2014]. Available from: http://www.mortality.org.

[12] Bover O, Melilla P. Migration in Spain: Historical Background and Migration in Spain: Historical Background and Current Trends. IZA; 1999.

[13] World Development Indicators; [cited 29 December 2014]. Available from: http://data.worldbank.org/indicator/SM.POP.NETM.

[14] Migrants in Europe. A statistical portrait of the first and second generation.; 2011 [cited 29 December 2014]. Available from: http://epp.eurostat.ec.europa.eu/cache/ITY_OFFPUB/KS-31-10-539/EN/KS-31-10-539-EN.PDF.

[15] Nardone A, de Ory F, Carton M, Cohen D, van Damme P, Davidkin I, et al. The comparative sero-epidemiology of varicella zoster virus in 11 countries in the European region. Vaccine 2007;25(45):7866–7872.

[16] García Cenoz M, Castilla J, Montes Y, Morán J, Salaberri A, Elía F, et al. Varicella and herpes zoster incidence prior to the introduction of systematic child vaccination in Navarre, 2005-2006. Anales del Sistema Sanitario de Navarra. 2007;30(1):71–80.

[17] Gilks WR. Markov Chain Monte Carlo. Wiley Online Library; 2005.

[18] UN World Population Prospects: The 2012 Revision; [cited 29 December 2014]. Available from: http://esa.un.org/unpd/wpp/index.htm.

[19] Brisson M, Melkonyan G, Drolet M, De Serres G, Thibeault R, De Wals P. Modeling the impact of one-and two-dose varicella vaccination on the epidemiology of varicella and zoster. Vaccine 2010;28(19):3385–3397.

[20] Poletti P, Melegaro A, Ajelli M, dal Fava E, Guzzetta G, Faustini L, et al. Perspectives on the impact of varicella immunization on Herpes Zoster. A model-based evaluation from three European countries. PLOS ONE 2013;8(4):e60732.

[21] Van Hoek AJ, Melegaro A, Zagheni E, Edmunds WJ, Gay N. Modelling the impact of a combined varicella and zoster vaccination programme on the epidemiology of varicella zoster virus in England. Vaccine. 2011;29:2411–2420.